ORIGINAL ARTICLE

High dose compressive loads attenuate bone mineral loss in humans with spinal cord injury

S. Dudley-Javoroski · P. K. Saha · G. Liang · C. Li · Z. Gao · R. K. Shields

Abstract

Summary People with spinal cord injury (SCI) lose bone and muscle integrity after their injury. Early doses of stress, applied through electrically induced muscle contractions, preserved bone density at high-risk sites. Appropriately prescribed stress early after the injury may be an important consideration to prevent bone loss after SCI.

Introduction Skeletal muscle force can deliver high compressive loads to bones of people with spinal cord injury (SCI). The effective osteogenic dose of load for the distal femur, a chief site of fracture, is unknown. The purpose of this study is to compare three doses of bone compressive loads at the distal femur in individuals with complete SCI who receive a novel stand training intervention.

Methods Seven participants performed unilateral quadriceps stimulation in supported stance [150% body weight (BW) compressive load—"High Dose" while opposite leg received 40% BW—"Low Dose"]. Five participants stood passively without applying quadriceps electrical stimulation to either leg (40% BW load—"Low Dose"). Fifteen participants performed no standing (0% BW load—"Untrained") and 14 individuals without SCI provided normative data. Participants underwent bone mineral density (BMD) assessment between one and six times over a 3-year training protocol.

Results BMD for the High Dose group significantly exceeded BMD for both the Low Dose and the Untrained groups ($p < 0.05$). No significant difference existed between the Low Dose and Untrained groups ($p > 0.05$), indicating that BMD for participants performing passive stance did not differ from individuals who performed no standing. High-resolution CT imaging of one High Dose participant revealed 86% higher BMD and 67% higher trabecular width in the High Dose limb.

Conclusion Over 3 years of training, 150% BW compressive load in upright stance significantly attenuated BMD decline when compared to passive standing or to no standing. High-resolution CT indicated that trabecular architecture was preserved by the 150% BW dose of load.

Keywords Bone density · Electrical stimulation · Muscle physiology · Quadriceps femoris · Spinal cord injury · Weight-bearing strengthening program

S. Dudley-Javoroski · R. K. Shields (✉)
Physical Therapy and Rehabilitation Science,
Carver College of Medicine, The University of Iowa,
1-252 Medical Education Building,
Iowa City, IA 52242-1190, USA
e-mail: richard-shields@uiowa.edu

P. K. Saha · G. Liang · C. Li · Z. Gao
Department of Electrical and Computer Engineering,
The University of Iowa,
Iowa City, IA 52242-1190, USA

P. K. Saha
Department of Radiology, Carver College of Medicine,
The University of Iowa,
Iowa City, IA 52242-1190, USA

Introduction

In paralyzed extremities, the absence of muscular contractions deprives the skeletal system of a critical stress necessary for bone health. As much as 50% of bone mineral may be lost at certain anatomic sites within the first 4 years post-injury [1]. Severe osteoporosis develops rapidly in people with spinal cord injury (SCI), leading to increased risk for fracture during routine daily activities [2]. A method to prevent the deterioration of the musculoskeletal system is essential to improve the health of people with SCI.

Although post-SCI osteoporosis has complex pathophysiology, the loss of mechanical stimuli to bone is considered to be a powerful contributor to BMD decline [3]. The reintroduction of load may therefore be a viable strategy for preventing or reducing bone loss after SCI. A large body of animal research has demonstrated the adaptive capacity of bone in response to mechanical loading. For human patients with SCI, inducing skeletal loads via muscle contractions offers the added advantage of a potential cardiovascular, metabolic, and cellular challenge to the deconditioned musculoskeletal system [4].

The formulation of muscle stimulation protocols to attenuate post-SCI BMD decline in humans has not been straightforward. Previous studies of passive standing [5], low-level electrical stimulation [6], body weight supported treadmill training [7], and electrically stimulated cycling [8, 9] revealed no BMD effects. However, mechanical loads delivered to the skeletal system during these studies were not estimated and may have been insufficient to exceed bone's hypothesized remodeling threshold [10]. More recently, cycling studies reported ~10–14% BMD increase at the distal femur [11, 12] or proximal tibia [13], but the dose of mechanical stress was not reported. The sites of BMD adaptations in these studies are typically rich in trabecular bone; the regions that have the greatest plastic potential [14] and the sites that are fractured most frequently in people with SCI [15].

We recently reported the long-term bone-sparing benefits of mechanical loads delivered to the tibia via isometric soleus muscle contractions [16–19]. Over greater than 3 years of unilateral training, BMD was spared in trained limbs (>30% between-limb difference) [16], chiefly along the line of action of the soleus muscular loads [20]. Modeled compressive loads during this study were ~1.5 times body weight. Using this knowledge, we developed a method to deliver a range of compressive loads to the lower extremity during upright stance in humans with SCI. We verified, through a biomechanical model, that the more dangerous shear forces [21] remain below 22% body weight (% BW) while the osteogenic compressive loads can exceed 150% BW during active-resisted stance [22]. Using this method, we are able to dose three levels of stress to the distal femur in humans with SCI.

The purpose of this study is to compare three doses of bone compressive loads: 0% BW (no standing), 40% BW with passive standing, and 150% BW induced by quadriceps stimulation during stance on BMD loss at the distal femur in individuals with complete SCI. A secondary objective is to explore bone loss at the proximal and distal tibia, sites marginally influenced by quadriceps muscle forces. The novelty of this study is that the dose of stress was estimated, the intervention is an activity that individuals with SCI enjoy (standing) [23], and the long-term impact of this intervention on bone plasticity was determined.

Methods

Subjects

The protocol was approved by the University of Iowa Human Subjects Office Institutional Review Board. All participants provided written informed consent before participating. Twenty-eight individuals with motor complete (AIS-A and B) [24] spinal cord injury participated in this study. Demographic data appear in Table 1. An additional 14 individuals without SCI served as a normative control condition. Exclusion criteria were a history of bone pathology (i.e., bone metabolic disease, cancer, etc.), thyroid disorder, previous fracture at the scan sites, pregnancy, and medications known to affect bone metabolism. Individuals without an SCI underwent a single bilateral assessment with peripheral quantitative computed tomography (pQCT). Bilateral values were averaged across limbs for each individual. Participants with SCI underwent between one and six bilateral pQCT scans.

Quadriceps training protocol

This study was conducted as a mixed cross-sectional and longitudinal design. SCI individuals 1–7 (Table 1) performed unilateral quadriceps stimulation in supported stance ("High Dose" loading) with the knee in 20° of flexion. The standing system is illustrated in Fig. 1. During initial visits to the laboratory, the participants developed tolerance for standing in a standing frame under the supervision of a physical therapist. The standing frame incorporated padded plates positioned against the anterior surface of the individual's knees. Velcro straps secured the knees against the plates. A force transducer (1500ASK-200; Interface, Scottsdale, AZ, USA) mounted in series with one plate measured the isometric knee extension force during unilateral quadriceps activation. Signals from the force transducer were amplified 500 times (Therapeutics Unlimited, Iowa City, IA, USA) and sampled at 2,000 Hz (Datapac 2K2; RUN Technologies, Mission Viejo, CA, USA). The experiment was controlled by custom-designed software, which directed digital pulses from a data-acquisition board (Metrabyte DAS 16F; Keithley Instruments Inc., Cleveland, OH, USA) housed in a microcomputer. The microcomputer output was conveyed via shielded cabling to a muscle stimulator unit (Digitimer model DS7A; Digitimer Ltd., Welwyn Garden City, Hertfordshire, UK). We delivered 60 100-pulse trains (20 Hz, 200 μs, up to 200 mA) to the quadriceps via reusable carbon adhesive electrodes. Each train was followed by 5 s of rest, yielding a 1:1 work/rest ratio. Participants performed two stimulation bouts separated by 5 min of rest during each training session.

Study participants initially traveled to the laboratory for quadriceps training sessions three times per week until

Table 1 Subject characteristics

Subject	Gender	SCI level	AIS	Age	Yrs post-SCI at first scan	pQCT time bins	Loading dose
1	M	T7	A	27	0.30	2–7	High
2	M	T4	A	16	0.38	1–3,5	High
3	M	T8	A	20	0.24	1,3,5	High
4	M	T10	A	37	0.22	1,4	High
5	M	T10	A	26	0.99	4–6	High
6	F	C5–6	A	26	1.50	5–6	High
7	M	T6	A	28	2.05	7	High
8	M	T12	A	39	0.21	1–2	Low
9	M	T8	B	43	0.33	2–4,6	Low
10	M	T8	A	38	0.53	3,4,6,7	Low
11	M	T11	A	34	0.68	3–5	Low
12	M	T4	A	44	0.61	3,4,6	Low
13	M	T8	A	19	0.19	1–2	N/A
14	M	C6	A	49	0.31	2	N/A
15	F	T6	A	18	0.41	2,7	N/A
16	M	T12	A	20	0.42	2–3	N/A
17	M	T11	A	22	0.81	4–6	N/A
18	M	T10	A	64	1.49	5	N/A
19	M	T6	A	34	1.77	6	N/A
20	M	T9	A	36	7.10	7	N/A
21	M	T4	A	24	3.20	7	N/A
22	M	T4	A	26	4.20	7	N/A
23	M	T3	A	47	19.00	7	N/A
24	M	T11	B	61	13.27	7	N/A
25	M	T1	A	49	24.23	7	N/A
26	M	T4	A	46	9.21	7	N/A
27	F	T6	A	44	23.04	7	N/A
28	F	T1	B	63	9.15	7	N/A
29	M			30			
30	M			24			
31	M			24			
32	F			22			
33	M			24			
34	M			42			
35	M			27			
36	M			23			
37	M			24			
38	M			30			
39	F			48			
40	F			31			
41	M			50			
42	M			28			

SCI spinal cord injury, *AIS* American Spinal Injury Association (ASIA) Impairment Scale (AIS), *pQCT* peripheral quantitative computed tomography. Time bin 1=0–0.25 year; time bin 2=0.25–0.50 year; time bin 3=0.50–0.75 year; time bin 4=0.75–1 year; time bin 5=1–1.5 years; time bin 6=1.5–2 years; time bin 7=>2 years

tolerance for upright positioning and for electrical stimulation were attained. At this point, individuals 1–5 and 7 received standing chairs and custom-designed stimulators to perform the training protocol at home. (Participant number 6 elected to do all training in the laboratory due to limited assistance available at home.) At-home training in the standing wheelchairs replicated the positioning and dose of training performed in the laboratory. A force transducer with full-contact padding measured quadriceps extension force at the popliteal fossa (Fig. 1). The custom-designed
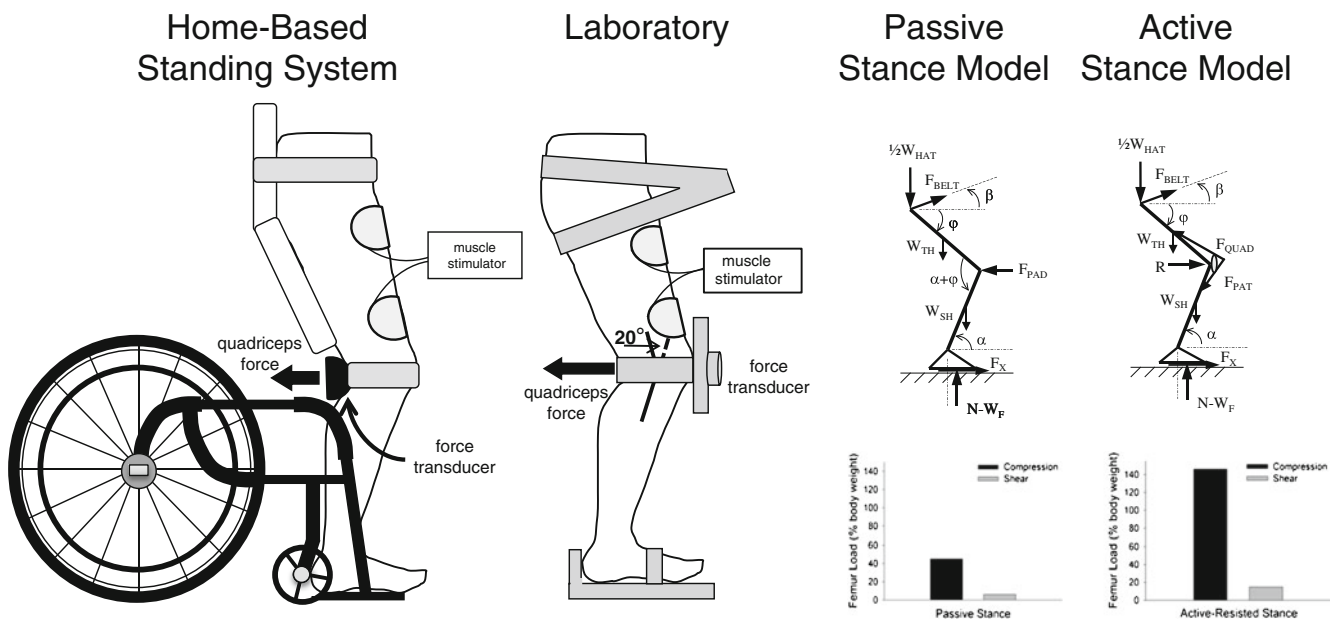
Home-Based Standing System

Laboratory

Passive Stance Model

Active Stance Model

Fig. 1 Schematic representation of the standing systems (left pair), and free body diagrams of the lower body during passive and active stance (right pair). In the stance models, each limb bears one half of the weight of the head, arm, and trunk segments ($\frac{1}{2}W_{HAT}$) plus the weight of the thigh (W_{TH}) and the weight of the shank (W_{SH}). During standing, thigh angle (φ)=71°, shank angle (α)=83°, and belt angle (β)=4°. The internal forces from the quadriceps and patellar tendons (F_{quad} and F_{pat}, respectively) in the active model replace the force of the supporting knee pad (F_{pad}) in the passive model

muscle stimulator logged the participant's training bouts with a date and time stamp that was downloadable at the laboratory. Study participants were asked to perform quadriceps training five times per calendar week via any combination of laboratory and at-home sessions.

Passive standing protocol

A second group of five individuals with SCI stood in a standing frame or a standing wheelchair without applying quadriceps electrical stimulation (Table 1, "Low Dose" loading cohort). We previously determined that modeled femur compressive loads during passive stance approximate 40% of body weight (% BW) (Fig. 1) [25]. Participants were requested to stand for 30 min on five calendar days per week. These individuals logged their training participation in notebooks.

In the High Dose group, the limb that did not receive electrical stimulation did perform passive stance during training sessions. Data from the untrained limbs of High Dose participants were therefore added to the Low Dose group.

Untrained subjects

A final group of 15 individuals with SCI served as a non-training group. These individuals performed no standing or electrical stimulation and underwent bone density assessment between one and three times (Table 1).

Rationale for training doses

Our previous work indicated that targeting five electrical stimulation sessions per week was sufficient to induce muscle physiology and bone mineral density adaptations in individuals with SCI [16, 18, 26]. In these studies, participants performed 83% of the requested training dose over a 3-year protocol [16]. We anticipated that a similar level of compliance would be attained by the present study cohort.

In the present study, we explore whether femur loads using a functional standing task at three "dose" levels can affect longitudinal BMD decline. To estimate loads during training, we developed a biomechanical model that derived distal femur compressive and shear forces at various levels of quadriceps activation (Fig. 1) [25]. Loads in the High Dose group were designed to replicate the 150% BW loads delivered in our previous soleus training protocol. Because passive stance is a functional activity commonly performed by individuals with SCI, we included a Low Dose group that routinely experienced passive loads of ~40% BW. Finally, because the standard of rehabilitation care in the USA does not include any form of standing, we enrolled a non-training cohort who performed no standing or electrical stimulation. Although these individuals' limbs undoubtedly experienced occasional loads via spasms or external forces, for all practical purposes the dose of load for this group was 0% BW.

Because the proximal and distal tibia are common fracture locations, we also elected to measure these sites because of their clinical importance [2].

pQCT scan procedure

pQCT measurements were performed with a Stratec XCT 3000 densitometer (Stratec Medical, Pforzheim, Germany). This device is calibrated with respect to fat (fat density= 0 mg/cm^3). Voxel size was 0.4 mm^3, scanner speed was 25 mm/s, and slice thickness was 2.2 mm.

Using a tape measure, femur and tibia length were measured using bony landmarks [27, 28]. An investigator passed the limb through the pQCT gantry and secured the individual's foot onto a footplate. Using an inclinometer placed just distal to the tibial tuberosity, the investigator adjusted the vertical height of the footplate in order to bring the pitch of the shank to horizontal. A radiology technician performed a scout view of the talocrural joint and placed a reference line at the distal limit of the tibia. Using this reference line, the scanner obtained an image at 4% of tibia length, measured from the distal end. Next, the radiology technician performed a scout view of the tibio-femoral joint and placed reference lines at the distal limit of the lateral femoral condyle and at the proximal limit of the tibial plateau. Using these reference lines, the scanner obtained an image at 12% of femur length and at 86% of tibia length (each measured from the distal end).

pQCT analysis procedures

For each image, an investigator defined a region of interest that incorporated a small amount of soft tissue outside of the periosteal margin. A threshold algorithm removed voxels below 200 mg/cm^3, starting from the outer edge of the region of interest and moving inward. This removed all voxels corresponding to muscle and fat and defined the periosteal edge. Inside the periosteal border, densities higher than 400 mg/cm^3 were defined as cortical/subcortical bone and values lower than this threshold were defined as trabecular bone. Cortical/subcortical voxels were excluded from further analysis. A 3×3 voxel filter then proofed the remaining image to detect pockets of high-density values. Voxels that had substantially higher BMD than the neighboring voxels were reassigned as subcortical bone and were excluded from further analysis. Trabecular BMD was obtained from the resulting image. Because the cortical shell is very thin at this site (and is therefore subject to the partial-volume effect [29]), we report only trabecular BMD.

Data processing

To facilitate longitudinal comparisons among cohorts, we partitioned the dataset into seven time bins based on time post-SCI: 0–0.25 years, 0.25–0.50 years, 0.50–0.75 years, 0.75–1 year, 1–1.5 years, 1.5–2 years, and >2 years. Mean (SD) BMD was computed for all individuals present in each time bin (see Table 1 for individual representation across time bins). Peak quadriceps force was computed for the High Dose cohort at these time bins. Quadriceps fatigue index (FI), the quotient of the force produced in the final and the first contractions, was likewise computed for the High Dose cohort. Quadriceps force for each participant was entered into a biomechanical model that calculated compression and shear at the distal femur (Fig. 1).

High-resolution CT

We identified one individual from the High Dose training cohort who demonstrated the greatest trained versus untrained within subject limb BMD difference (subject number 1, Table 1). This participant underwent high-resolution multi-detector CT imaging (Definition Flash; Siemens Healthcare, Erlangen, Germany) of both limbs to explore whether the dose of training preserved trabecular architecture of the distal femur. We also scanned the proximal and distal tibiae to determine whether passive stance affected trabecular architecture. Both knees were scanned using a single source spiral acquisition which utilized a 16×0.3 mm detector collimation, 120 kVp, 240 mAs, 1.0 pitch, and a gantry rotation speed of 1.0 s. After scanning both knees in a helical mode with a 0.4-mm slice thickness, data were reconstructed at 0.3-mm slice thickness using a normal cone beam method with a special U70u kernel achieving high structural resolution. Images were processed using volumetric topologic analysis (VTA) [30]. This method classifies trabeculae on a continuum between plates (width ~1.5 mm) and rods (width ~0.15 mm), facilitating early detection of the plate-to-rod conversion known to occur in osteoporosis [31]. After registration between the left and right limbs, ten matching axial regions spanning the most distal 20% of the femora, the most proximal 20% of the tibiae, and the most distal 20% of the tibiae were defined (2% per segment). A 25% radial peel mode was applied on axial regions to exclude cortical bone in the measurements. Architectural parameters compared between limbs included trabecular surface width (SW, microns) and the surface-to-curve ratio (SCR), an index of relative "plateness" of a trabecular region [30]. A low SCR indicates extensive erosion of plates and conversion to rods. The INTable™ Calibration Phantom Couch Pad was scanned together with the participant and used to calibrate CT Hounsfield units into volumetric BMD (mg/cm^3).

Statistical analysis

Quadriceps force and fatigue index and modeled femur compressive loads for the High Dose group were each analyzed using a one-way analysis of variance (ANOVA) across the seven time bins. Pairwise multiple comparisons (Tukey) were used when indicated. Significance was set to alpha <0.05.

Previous reports suggest that at the distal femur, BMD reaches a steady-state value at approximately 4.1 years post-SCI [32, 33]. To determine whether participants with chronic SCI demonstrated steady-state BMD, we partitioned individuals in the final time bin (>2 years SCI) into two sub-cohorts divided before and after 4.1 years. We used a one-way ANOVA to determine whether BMD differed before versus after this hypothesized steady-state time.

To examine early effects of training, we pooled data from 0.5 to 1 year post-injury ("Year 1" measurement). To examine later effects of training, we pooled data from 1.5 to 3 years ("Year 3" measurement). We used a two-way (group × time) ANOVA to compare BMD differences among the High Dose, Low Dose, and Untrained groups at these two time points. Pairwise multiple comparisons (Tukey) were used when indicated. Significance was set to alpha <0.05.

All high-resolution CT results for the trained and untrained limb of one participant are presented descriptively.

Results

Training compliance, muscle adaptations, and target femur compressive doses

Individuals in the High Dose group completed 67.6% of the requested training bouts, on average (approximately three sessions per calendar week). Low Dose trainers completed 66.0% of the requested training bouts. Longitudinal quadriceps peak force and fatigue index data for the High Dose group appear in Fig. 2a–b. A significant main effect of time post-SCI was present for both force and FI ($p=0.003$ and $p=0.015$). Follow-up tests revealed no significant differences between individual time bins (all comparisons $p>0.05$). Modeled femur compressive loads are shown in Fig. 2c. The target dose of load (150% BW) was attained between 0.5 and 0.75 years of training. A significant main effect of time post-SCI was present ($p=0.003$). Follow-up tests revealed that compressive load for the final time bin (>2 years) was significantly higher than for the first time bin (0.25 year) ($p=0.044$).

Longitudinal bone density dose–response

Distal femur BMD data for all time bins appear in Fig. 3a. Data for the untrained and Low Dose groups are illustrated together. The slope of BMD loss across time for the Low Dose and Untrained limbs was more than three times higher than for the High Dose limbs. For limbs >2 years post-SCI, BMD did not differ before the predicted steady state (2 to 4.1 years) and after the predicted steady state (4.1 to 24 years, mean 10.17 years) ($p=0.588$).

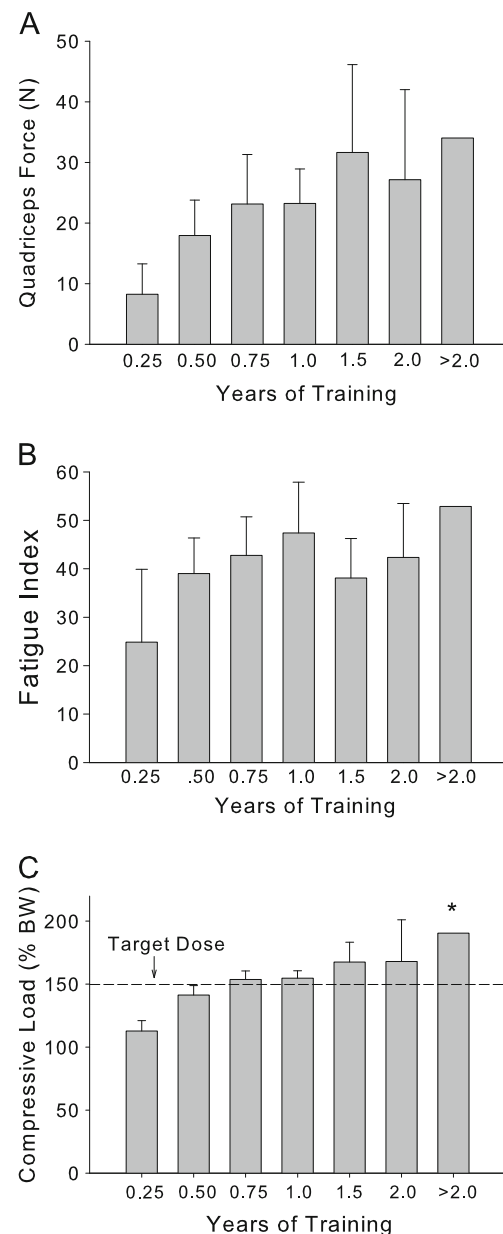Proximal tibia BMD data for all time bins appear in Fig. 3b. The slope of BMD loss across time for the Low

Fig. 2 Quadriceps adaptations to High Dose training. One-way ANOVA revealed a significant effect of training duration for quadriceps force ($p=0.003$), fatigue index ($p=0.015$), and for femur compressive load ($p=0.003$). *Significantly different from time bin 1 (0.25 year) ($p=0.044$)

Dose and Untrained limbs was 25.1% higher than the slope for High Dose limbs. Unlike the distal femur, no steady-state BMD duration has yet been reported for the proximal tibia. Using the distal femur steady-state estimate, BMD did not differ before the predicted steady state (2 to 4.1 years) and after the predicted steady state (4.1 to 24 years, mean 10.17 years) ($p=0.315$).

Distal tibia BMD data for all time bins appear in Fig. 3c. The slope of BMD loss across time for the Low Dose and Untrained limbs was 14.4% lower than the slope for High
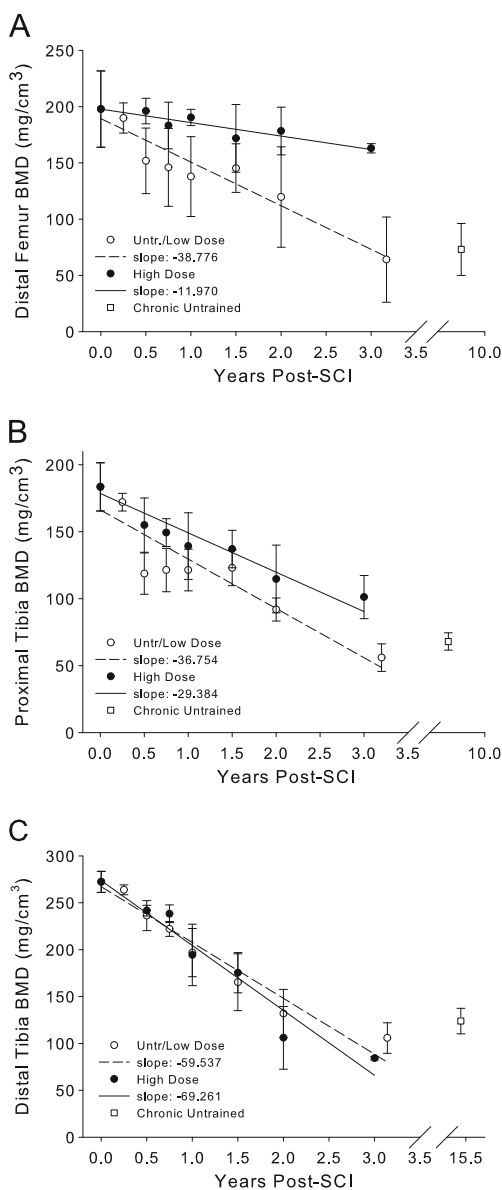
2341

Fig. 3 Longitudinal peripheral quantitative computed tomography (pQCT)-derived bone mineral density (BMD) for the distal femur (a), proximal tibia (b), and distal tibia (c). Untrained and Low Dose limbs are plotted together
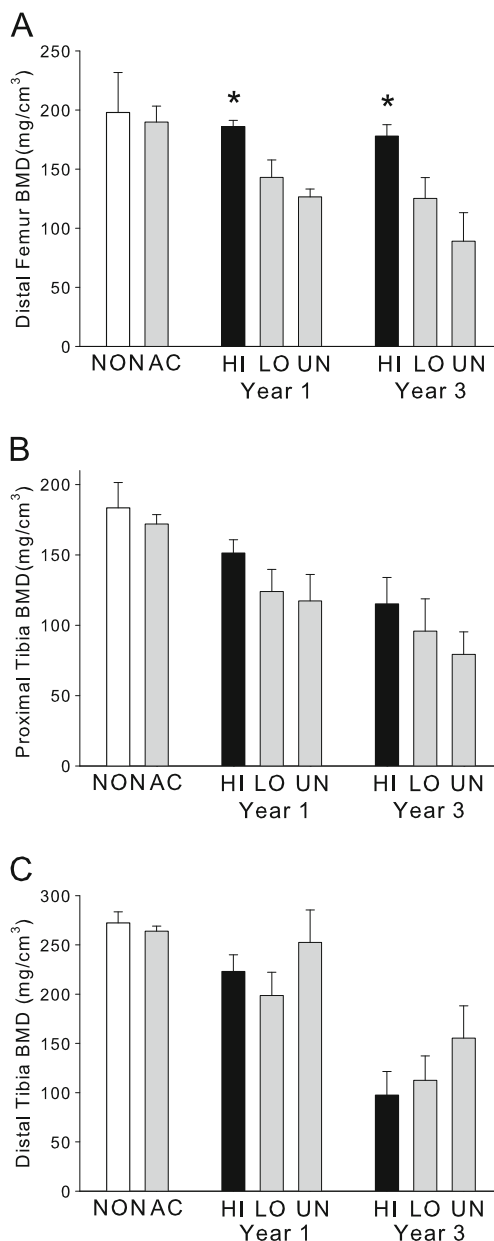

Fig. 4 Longitudinal peripheral quantitative computed tomography (pQCT)-derived bone mineral density (BMD) at the year 1 and year 3 measurement points for the distal femur (a), proximal tibia (b), and distal tibia (c). *NON* non-spinal cord injury (SCI), *AC* acute SCI (<3 months), *HI* High Dose cohort, *LO* Low Dose cohort, *UN* Untrained cohort. *Significantly greater than LO and UN ($p<0.019$)

Dose limbs. Steady-state BMD duration for the distal tibia has previously been reported to be 6.8 years [32]. For limbs >2 years post-SCI, BMD did not differ before the predicted steady state (2 to 6.8 years) and after the predicted steady state (6.8 to 24 years, mean 15.39 years) ($p=0.185$).

Figure 4 depicts BMD grouped into the year 1 and year 3 measurements. To ensure fair comparisons, time post-SCI was similar among the High Dose, Low Dose, and Untrained conditions (0.80, 0.79, and 0.74 years for the year 1 measurement; 2.19, 2.24, and 2.27 years for the year 3 measurement). For the distal femur (Fig. 4a), a two-way (group × time) ANOVA indicated a significant main effect

of dose cohort ($p=0.003$), with BMD for the High Dose group significantly exceeding BMD for both the Low Dose and the Untrained groups ($p=0.003$ and $p=0.019$). No significant difference existed between the Low Dose and Untrained groups ($p=0.353$), indicating that BMD for individuals performing passive stance did not differ from individuals who performed no standing. At year 1, pooled distal femur BMD for the Low Dose and Untrained limbs was 74.9% of the High Dose value, a 25.1% difference. At year

3, pooled distal femur BMD for the Low Dose and Untrained limbs was 61.1% of the High Dose value, a 38.9% difference.

For the proximal tibia (Fig. 4b), a two-way (group × time) ANOVA indicated no effect of dose group ($p=0.220$) but a significant main effect of time (year 1 > year 3, $p<0.041$). At year 1, pooled proximal tibia BMD for the Low Dose and Untrained limbs was 79.0% of the High Dose value. At year 3, pooled BMD for Low Dose and Untrained limbs was 77.4% of the High Dose value.

For the distal tibia (Fig. 4c), a two-way (group × time) ANOVA indicted no effect of dose cohort ($p=0.246$) but a significant main effect of time (year 1 > year 3, $p<0.001$). At year 1, pooled distal tibia BMD for the Low Dose and Untrained limbs was 94.5% of the High Dose value. At year 3, pooled BMD for Low Dose and Untrained limbs was 137.5% of the High Dose value.

High-resolution CT: within-subject dose effect

Figure 5 depicts the CT cross-sectional images (a, b) from subject number 1's trained and untrained limb 12% femur sites. In a single CT slice, the loss of trabecular elements within the untrained limb can be observed visually. Figure 5c and d show a three-dimensional reconstruction of each distal femur with a cylindrical region of interest highlighted for further inspection. Figure 5e and f show the VTA-reconstructed trabecular lattice contained within each region of interest, illustrating the loss of trabecular elements and relative absence of plates on the untrained side.

Figure 6 shows CT-derived BMD and trabecular architecture values obtained from regions 2–9 of the individual's segmented femur and tibia images. Over the sampled region, mean CT-derived BMD for the trained distal femur was 119.46 mg/cm^3. BMD for the contralateral untrained side was 16.54 mg/cm^3, just 13.9% of the trained limb value. Training effects were likewise apparent in the femur trabecular architecture parameters; untrained limb surface width and surface-to-curve ratio were just 32.5% and 9.6% of the trained limb values, respectively.

Between-limb differences were smaller but still apparent at the proximal tibia. From the longitudinal pQCT database, proximal tibia BMD for this individual was 5% higher for the "untrained" than the "trained" side. In contrast, CT-derived mean BMD of the "untrained" proximal tibia was just 23.0% of the "trained" side. Surface width and surface-to-curve ratio were likewise lower in the "untrained" limb (55.4% and 27.8% of the "trained" side, respectively). At the distal tibia, pQCT-derived BMD for this individual's "untrained" side was 82.5% of the "trained" limb value. As measured by CT, BMD, SW, and SCR of the "untrained" limb were 44.9%, 83.8%, and 65.7% of the "trained" limb values, respectively.
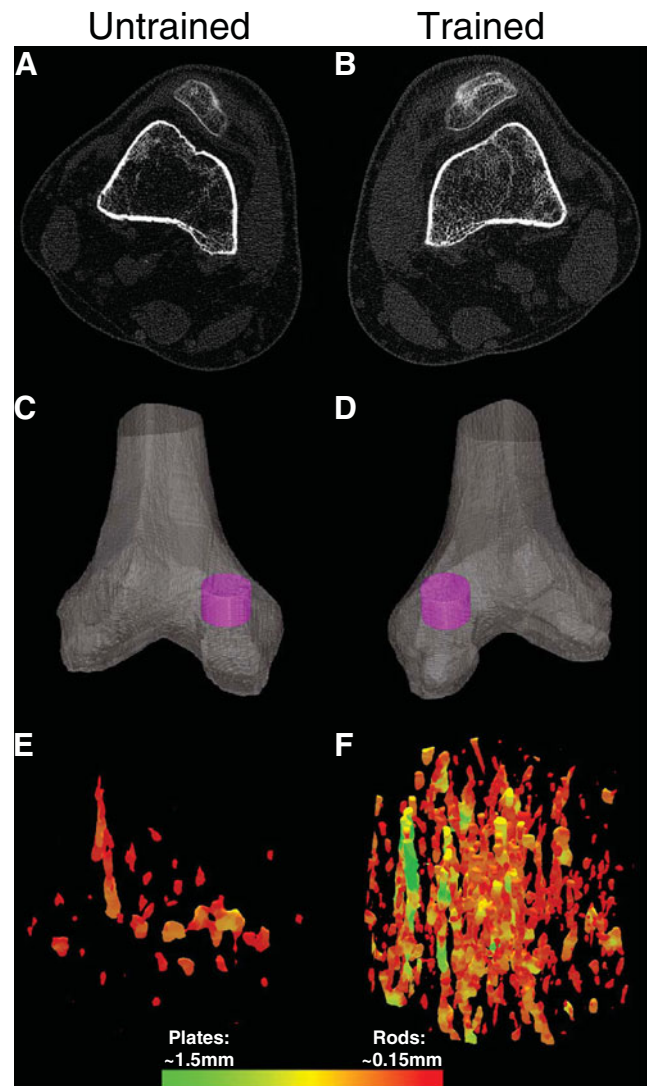

Fig. 5 Representative example of CT images from a subject in the High Dose cohort. Images in the *left-hand column* are from the subject's untrained limb. Images from the *right-hand column* are from the subject's trained limb. **a**, **b** Cross-sectional CT images at the 12% femur sites. **c**, **d** Cylindrical regions of interest within each medial femoral condyle. **e**, **f** Three-dimensional reconstruction of the trabecular lattice within each region of interest. The *color scale* corresponds to voxels assigned as plates and rods during volumetric topologic analysis (VTA). The maximum and minimum dimensions of plates and rods are listed

Discussion

The purpose of this study was to compare post-SCI BMD of the distal femur in individuals with complete SCI who receive three doses of bone compressive loads: 0% BW (no standing), 40% BW with passive standing, and 150% BW with quadriceps activation in stance. Quadriceps loading during stance yielded significantly higher BMD over 3 years of training than the lower dose levels. No significant differences emerged between passive standing (Low Dose) and no standing
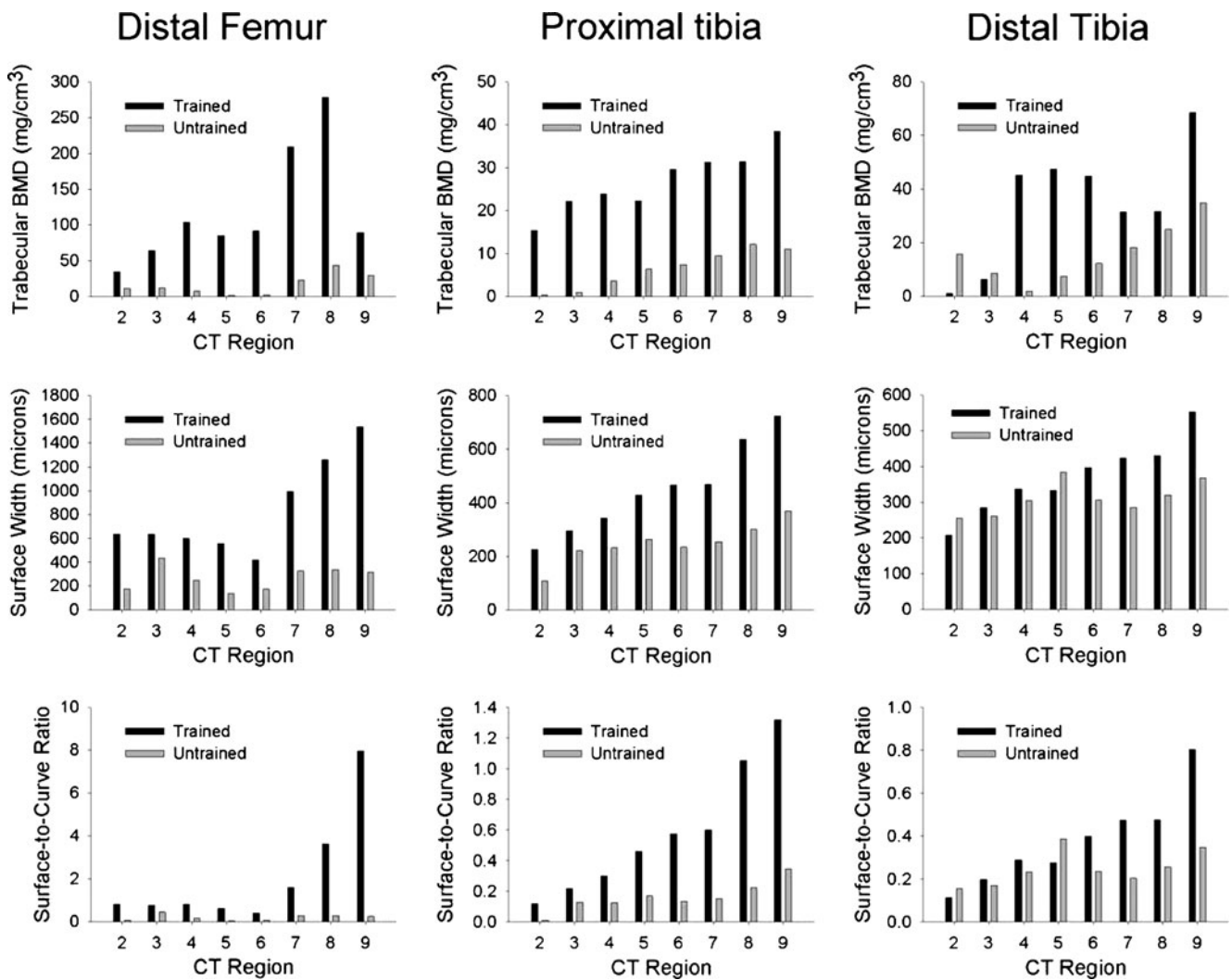
Fig. 6 CT-derived bone mineral density (BMD) (*top row*), trabecular surface width (*middle row*), and trabecular surface-to-curve ratio (*bottom row*) from a subject in the High Dose cohort

activity. In a single subject, training effects at the tibia sites were not detectable by pQCT but were apparent with high-resolution CT imaging. The results of this study confirm that muscular loads in stance offer a bone-sparing stimulus to the distal femur, a common fracture site after SCI.

Adaptations to loading dose

Study participants in the High Dose group showed rapid adaptations in quadriceps physiology during training. Quadriceps force doubled between 0.25 and 0.5 year due to a combination of training adaptations and gradual intensification of stimulus intensity as the participants acclimated to the protocol. Quadriceps fatigue index showed a similar trend, with the greatest gains in the first 6 months of training. Quadriceps force and fatigue index adaptations were maintained for the duration of training.

The results of the present study support that post-SCI BMD decline can be attenuated with routine application of mechanical loads that meet certain dose criteria (150% BW compressive load). A key feature of this study is that the compressive load and shear loads delivered during training had been estimated via biomechanical modeling [25]. A drawback of many previous human studies has been that loading conditions were not specified, limiting the ability to interpret the optimal dose of stress necessary to adapt bone. A chief example of this issue is that some [11–13, 34–36] but not all [9, 37] studies of electrically assisted cycling studies reported effects upon BMD. Factors contributing to the success or failure of these interventions are difficult to ascertain, as the dose of stress was not reported. Although cycling power output has been noted as a factor determining bone adaptations [11], the links between cycling power, muscle force, and estimated skeletal loads are modified by the force–velocity relationship of skeletal muscle. High

cycling power output does not necessarily indicate high muscle forces because high power may be achieved by a high cadence (velocity) with low accompanying muscular/skeletal loads. The actual loading conditions delivered during cycle training require further investigation to better understand the dose–response issues.

Biomechanical estimation of loading conditions may be more straightforward in training protocols that involve single-joint systems. Open kinetic chain knee extension against resistance (seated knee extension against load) has been shown to attenuate early BMD loss at the distal femur and proximal tibia [38] and to increase BMD at these sites in individuals with chronic SCI [39]. However, shear forces at the distal femur are high when the knee is flexed during quadriceps contraction [25], yielding a risk for fracture [40]. The supported-stance intervention used in the present study limits shear forces to <22% BW during administration of the targeted 150% BW compressive load [25]. The long-term BMD adaptations observed with this dose of training (38.9% at 3 years) were commensurate with the adaptations observed in our previous long-term single segment soleus/tibia loading protocol (35.4% at 3 years) [20] that used the same target dose of skeletal load.

A lower dose of skeletal load (40% BW; passive stance) did not offer a statistically significant BMD-sparing benefit at year 1 or year 3 of the training protocol for the distal femur, the proximal tibia, or the distal tibia (Fig. 4). The efficacy of passive stance for preserving BMD is an area of controversy. Two recent studies suggest that individuals who routinely stand experience less BMD loss over time than individuals who perform no standing [41, 42]. However, at least some of these study participants ambulated with leg braces [42], a scenario that likely exposes the limbs to ground reaction forces and impact loads that exceed stationary passive stance. Other studies have found no correlation between passive standing and bone status [43], and no efficacy of passive stance to reduce bone decline [5]. Although our data do not support a strong passive stance influence on bone density, other benefits of standing for seated pressure relief, bowel and bladder function, and psychological well-being suggest other benefits that are not related to bone loss [44]. Importantly, there were descriptive trends suggesting that passive loading may have an anti-osteoporotic effect, albeit small, when compared to an untrained limb (Fig. 4a, b).

Detection of training effects

We have previously noted that BMD varies from distal to proximal in the tibia and femur distal epiphyses [27, 28] and that adaptations to mechanical loading may occur in asymmetric patterns [20]. No previous study has determined the optimal pQCT scan site for detecting bone adaptations to

mechanical loading. In the present study, CT imaging of the distal femur of one individual who trained one leg suggests that our 12% femur pQCT slice location (approximately region 6 in Fig. 6) may underestimate training adaptations that occur at slightly more proximal sites (regions 7 and 8, approximately 14–16% of femur length). In addition, the single pQCT image at 12% of femur length suggested that untrained femur BMD was 65.42% of the trained limb value. Using CT to sample a greater anatomic range revealed that untrained limb BMD was just 13.85% of the trained limb value overall. CT also revealed a considerable training effect at the proximal tibia (~77% difference between limbs) that was not as apparent by the single pQCT slice at 86% of tibia length. The pattern of bone preservation and loss is likely to vary considerably among participants with different anatomic characteristics. To ensure that bone adaptations to various doses of stress are detected, further work with high-resolution imaging is necessary to identify the locations that are most sensitive to change across time.

Trabecular architecture adaptations

The longitudinal BMD decline observed in the pQCT database reflects the accumulated deterioration and destruction of trabecular elements. Trabecular thinning that remains below the limit of measurement resolution of pQCT will not yield measurable BMD loss. Measuring trabecular architecture characteristics directly via high-resolution CT may allow bone adaptations to be detected more rapidly. The present study establishes the presence of training-related differences in trabecular architectural features in an individual with known BMD training effects. We are not aware of previous studies that establish normative SW and SCR values for the sites sampled in this participant. One previous study indicated that SCR of the distal tibia in women with post-menopausal osteoporosis was ~5.1 [31]. Our participant's SCR values at the distal tibia were <1.0 for both limbs, suggesting extensive conversion of trabecular plates to rods. At the femur, between-limb differences in SW and SCR were large (77% and 91%, respectively), suggesting that High Dose training limited the conversion of plates to rods at this site. Preventing the conversion of trabecular plates to trabecular rods may be associated with improved bone strength and decreased fracture risk [31, 45].

Clinical implications and limitations

The extensive BMD-sparing effect of the High Dose load at the femur was less apparent at more distal skeletal sites. (Despite CT evidence of adaptations in a single participant, BMD of the cohort still declined rapidly at the tibial sites; Fig. 3.) This finding is not surprising, as loads induced by muscle contractions are most concentrated over the bony

sites that the muscle spans. In this study, the quadriceps muscle was activated, which generated the primary stress through the distal femur during stance. Because sites throughout the lower extremity are at risk for fracture, more research with alternative methods (including additional muscles being activated) are necessary before active stance becomes a comprehensive method to attenuate bone loss in people with SCI.

Conclusions

Over 3 years of training, a high dose of compressive load (150% BW) administered via quadriceps activation in stance significantly attenuated BMD decline at the distal femur when compared to a low dose of load (passive standing) or no loading (no standing) in subjects with SCI. High-resolution CT imaging supports that the high dose compressive load training attenuated trabecular architecture deterioration and that training adaptations occurred in the tibia of the trained limb. Future studies are needed to determine the long-term efficacy of various limb loading methods to prevent osteoporosis in people with SCI.

References

1. Eser P, Frotzler A, Zehnder Y, Wick L, Knecht H, Denoth J, Schiessl H (2004) Relationship between the duration of paralysis and bone structure: a pQCT study of spinal cord injured individuals. Bone 34:869–880
2. Fattal C, Mariano-Goulart D, Thomas E, Rouays-Mabit H, Verollet C, Maimoun L (2011) Osteoporosis in persons with spinal cord injury: the need for a targeted therapeutic education. Arch Phys Med Rehabil 92:59–67
3. Lanyon LE (1996) Using functional loading to influence bone mass and architecture: objectives, mechanisms, and relationship with estrogen of the mechanically adaptive process in bone. Bone 18:37S–43S
4. Davis GM, Hamzaid NA, Fornusek C (2008) Cardiorespiratory, metabolic, and biomechanical responses during functional electrical stimulation leg exercise: health and fitness benefits. Artif Organs 32:625–629
5. Ben M, Harvey L, Denis S, Glinsky J, Goehl G, Chee S, Herbert RD (2005) Does 12 weeks of regular standing prevent loss of ankle mobility and bone mineral density in people with recent spinal cord injuries? Aust J Physiother 51:251–256
6. Clark JM, Jelbart M, Rischbieth H, Strayer J, Chatterton B, Schultz C, Marshall R (2007) Physiological effects of lower extremity functional electrical stimulation in early spinal cord injury: lack of efficacy to prevent bone loss. Spinal Cord 45:78–85
7. Giangregorio LM, Hicks AL, Webber CE, Phillips SM, Craven BC, Bugaresti JM, McCartney N (2005) Body weight supported treadmill training in acute spinal cord injury: impact on muscle and bone. Spinal Cord 43:649–657
8. Leeds EM, Klose KJ, Ganz W, Serafini A, Green BA (1990) Bone mineral density after bicycle ergometry training. Arch Phys Med Rehabil 71:207–209
9. BeDell KK, Scremin AM, Perell KL, Kunkel CF (1996) Effects of functional electrical stimulation-induced lower extremity cycling on bone density of spinal cord-injured patients. Am J Phys Med Rehabil 75:29–34
10. Frost HM (2003) Bone's mechanostat: a 2003 update. Anat Rec 275A:1081–1101
11. Bloomfield SA, Mysiw WJ, Jackson RD (1996) Bone mass and endocrine adaptations to training in spinal cord injured individuals. Bone 19:61–68
12. Frotzler A, Coupaud S, Perret C, Kakebeeke TH, Hunt KJ, Donaldson Nde N, Eser P (2008) High-volume FES-cycling partially reverses bone loss in people with chronic spinal cord injury. Bone 43:169–176
13. Mohr T, Podenphant J, Biering-Sorensen F, Galbo H, Thamsborg G, Kjaer M (1997) Increased bone mineral density after prolonged electrically induced cycle training of paralyzed limbs in spinal cord injured man. Calcif Tissue Int 61:22–25
14. Snyder WS (ed) (1975) Report of the task group on reference man. Pergamon, Oxford
15. Eser P, Frotzler A, Zehnder Y, Denoth J (2005) Fracture threshold in the femur and tibia of people with spinal cord injury as determined by peripheral quantitative computed tomography. Arch Phys Med Rehabil 86:498–504
16. Shields RK, Dudley-Javoroski S (2006) Musculoskeletal plasticity after acute spinal cord injury: effects of long-term neuromuscular electrical stimulation training. J Neurophysiol 95:2380–2390
17. Shields RK, Dudley-Javoroski S, Frey Law L (2006) Electrically-induced muscle contractions influence bone density decline after spinal cord injury. Spine 31:548–553
18. Shields RK, Dudley-Javoroski S, Littmann AE (2006) Post-fatigue potentiation of paralyzed soleus muscle: evidence for adaptation with long-term electrical stimulation training. J Appl Physiol 101:556–565
19. Shields RK, Dudley-Javoroski S (2006) Musculoskeletal adaptation in chronic spinal cord injury: effects of long-term soleus electrical stimulation training. J Neurorehabil Neural Repair 21:169–179
20. Dudley-Javoroski S, Shields RK (2008) Asymmetric bone adaptations to soleus mechanical loading after spinal cord injury. J Musculoskelet Neuronal Interact 8:227–238
21. Zioupos P, Gresle M, Winwood K (2008) Fatigue strength of human cortical bone: age, physical, and material heterogeneity effects. J Biomed Mater Res A 86:627–636
22. Dudley-Javoroski S, Littmann AE, Chang SH, McHenry CL, Shields RK (2011) Enhancing muscle force and femur compressive loads via feedback-controlled stimulation of paralyzed quadriceps in humans. Arch Phys Med Rehabil 92:242–249
23. Shields RK, Dudley-Javoroski S (2005) Monitoring standing wheelchair use after spinal cord injury: a case report. Disabil Rehabil 27:142–146
24. American Spinal Injury Association (2002) International standards for neurological classification of SCI. American Spinal Injury Association, Atlanta

25. Frey Law L, Shields RK (2004) Femoral loads during passive, active, and active-resistive stance after spinal cord injury: a mathematical model. Clin Biomech 19:313–321

26. Dudley-Javoroski S, Shields RK (2008) Dose estimation and surveillance of mechanical loading interventions for bone loss after spinal cord injury. Phys Ther 88:387–396

27. Dudley-Javoroski S, Shields RK (2010) Longitudinal changes in femur bone mineral density after spinal cord injury: effects of slice placement and peel method. Osteoporos Int 21:985–995

28. Shields RK, Dudley-Javoroski S, Boaldin KM, Corey TA, Fog DB, Ruen JM (2006) Peripheral quantitative computed tomography: measurement sensitivity in persons with and without spinal cord injury. Arch Phys Med Rehabil 87:1376–1381

29. Hangartner TN, Gilsanz V (1996) Evaluation of cortical bone by computed tomography. J Bone Miner Res 11:1518–1525

30. Saha PK, Xu Y, Duan H, Heiner A, Liang G (2010) Volumetric topological analysis: a novel approach for trabecular bone classification on the continuum between plates and rods. IEEE Trans Med Imaging 29:1821–1838

31. Wehrli FW, Ladinsky GA, Jones C et al (2008) In vivo magnetic resonance detects rapid remodeling changes in the topology of the trabecular bone network after menopause and the protective effect of estradiol. J Bone Miner Res 23:730–740

32. Eser P, Schiessl H, Willnecker J (2004) Bone loss and steady state after spinal cord injury: a cross-sectional study using pQCT. J Musculoskelet Neuronal Interact 4:197–198

33. Frotzler A, Berger M, Knecht H, Eser P (2008) Bone steady-state is established at reduced bone strength after spinal cord injury: a longitudinal study using peripheral quantitative computed tomography (pQCT). Bone 43:549–555

34. Lai CH, Chang WH, Chan WP, Peng CW, Shen LK, Chen JJ, Chen SC (2010) Effects of functional electrical stimulation cycling exercise on bone mineral density loss in the early stages of spinal cord injury. J Rehabil Med 42:150–154

35. Lauer RT, Smith BT, Mulcahey MJ, Betz RR, Johnston TE (2011) Effects of cycling and/or electrical stimulation on bone mineral density in children with spinal cord injury. Spinal Cord 49:917–923

36. Ashe MC, Eng JJ, Krassioukov AV, Warburton DE, Hung C, Tawashy A (2010) Response to functional electrical stimulation cycling in women with spinal cord injuries using dual-energy X-ray absorptiometry and peripheral quantitative computed tomography: a case series. J Spinal Cord Med 33:68–72

37. Eser P, de Bruin ED, Telley I, Lechner HE, Knecht H, Stussi E (2003) Effect of electrical stimulation-induced cycling on bone mineral density in spinal cord-injured patients. Eur J Clin Investig 33:412–419

38. Groah SL, Lichy AM, Libin AV, Ljungberg I (2010) Intensive electrical stimulation attenuates femoral bone loss in acute spinal cord injury. PM&R 2:1080–1087

39. Belanger M, Stein RB, Wheeler GD, Gordon T, Leduc B (2000) Electrical stimulation: can it increase muscle strength and reverse osteopenia in spinal cord injured individuals? Arch Phys Med Rehabil 81:1090–1098

40. Hartkopp A, Murphy RJ, Mohr T, Kjaer M, Biering-Sorensen F (1998) Bone fracture during electrical stimulation of the quadriceps in a spinal cord injured subject. Arch Phys Med Rehabil 79:1133–1136

41. Alekna V, Tamulaitiene M, Sinevicius T, Juocevicius A (2008) Effect of weight-bearing activities on bone mineral density in spinal cord injured patients during the period of the first two years. Spinal Cord 46:727–732

42. Dionyssiotis Y, Lyritis GP, Mavrogenis AF, Papagelopoulos PJ (2011) Factors influencing bone loss in paraplegia. Hippokratia 15:54–59

43. Eser P, Frotzler A, Zehnder Y, Schiessl H, Denoth J (2005) Assessment of anthropometric, systemic, and lifestyle factors influencing bone status in the legs of spinal cord injured individuals. Osteoporos Int 16:26–34

44. Eng JJ, Levins SM, Townson AF, Mah-Jones D, Bremner J, Huston G (2001) Use of prolonged standing for individuals with spinal cord injuries. Phys Ther 81:1392–1399

45. Kleerekoper M, Villanueva AR, Stanciu J, Rao DS, Parfitt AM (1985) The role of three-dimensional trabecular microstructure in the pathogenesis of vertebral compression fractures. Calcif Tissue Int 37:594–597